


Nonuniversal aging during phase separation with long-range interaction

Soumik Ghosh  and Subir K. Das ^{*}

*Theoretical Sciences Unit and School of Advanced Materials,
Jawaharlal Nehru Centre for Advanced Scientific Research, Jakkur P.O., Bangalore 560064, India*

 (Received 27 July 2023; revised 5 February 2024; accepted 11 April 2024; published 6 May 2024)

Issues concerning the kinetics of phase transitions are not well established for the cases where the order parameter remains conserved with time, particularly when the interatomic interactions are long-range in nature. Here we present results on structure, growth, and aging from Monte Carlo simulations of the two-dimensional long-range Ising model. In our computer simulations, random initial configurations, for 50 : 50 compositions of up and down spins, mimicking high-temperature equilibrium states, have been quenched to temperatures inside the coexistence curve. Our analyses of the simulation data, for such a protocol, show interesting dependence of the aging exponent, λ , on σ , the parameter, within the Hamiltonian, that controls the range of interaction. These nonuniversal values of λ are compared with a theoretical result for lower bounds. For this purpose, we extracted information on relevant aspects of structural properties during the evolution. To estimate λ , as is necessary, we also calculated the average domain size and analyzed its time dependence to obtain the growth exponent α which also is nonuniversal. The trends in the values of λ and α , as well as an anomaly in structure, suggest that a crossover from the long-range to the short-range variety occurs at $\sigma \simeq 1$. The location of this boundary and the nonuniversality provide a picture that is surprisingly different from that of the corresponding static critical phenomena. Furthermore, our results suggest an important scaling law combining α and λ .

DOI: [10.1103/PhysRevE.109.L052102](https://doi.org/10.1103/PhysRevE.109.L052102)

In the literature of phase transitions, certain important questions are by concerning universality in far-from-equilibrium dynamics [1]. An objective there [1] is to understand relaxation within a system following its quench from a homogeneous region to an ordered or a phase-separated region of a phase diagram. During this process, interesting patterns, consisting of domains rich or poor in specific components, form, and their average size ℓ grows with time (t) as [1] $\ell \sim t^\alpha$. Alongside estimating this, another fundamentally important but more challenging task is to quantify the scaling behavior of relaxations starting from different ages, following the perturbation [2]. Such aging phenomena is often studied via the autocorrelation function [2–12] $C_{ag}(t, t_w) = \langle \psi(\vec{r}, t)\psi(\vec{r}, t_w) \rangle - \langle \psi(\vec{r}, t) \rangle \langle \psi(\vec{r}, t_w) \rangle$. Here ψ is a space (\vec{r}) and time-dependent order parameter, with t_w ($\leq t$) representing the waiting time, also referred to as the age of the system. The scaling decay of C_{ag} , to be detailed later, as a function of ℓ is quantified by an exponent λ . The values of α and λ take part in characterizing universality in kinetics of phase transitions [1,2,7,10].

In static critical phenomena, alongside a few other details, the range of the interaction decides classes of universality [13]. It is expected, though there will be two classes, above and below a certain cutoff for the range of interaction, in each of these the critical exponents will have values independent of further “micro” variations of the interaction range. Investigations of such features are of much fundamental and practical importance for nonequilibrium dynamics as well [12,14–19].

A question arises if, within the same model framework, the above-mentioned universality picture remains unchanged, i.e., whether the interaction-range boundary between the two dynamic classes is the same as in the static case, and unique sets of exponents define growth and aging phenomena on the two sides, irrespective of the distance from the boundary. However, unlike the case of critical phenomena, corresponding progress for evolution dynamics is limited, though important.

Even for the simple Ising model (IM), there exist serious computational challenges for the long-range (LRIM) variety [12,16–20], particularly for the case of the conserved order-parameter. Only two computational studies [16,21] investigated this case, reporting results *only* on α . Here, our primary focus is aging on which we present results on λ , for the conserved LRIM, covering a wide variation in the interaction range. It appears that λ has an interesting dependence on the latter. We also revisit the issue of growth and present computational results on such a nonuniversal feature in α from direct estimation. The overall picture is strikingly different from the corresponding static case, in terms of universality as well as shifting of the above-mentioned boundary. The values of λ are discussed against a theoretical bound [4] to facilitate which we analyze the structural properties that also, interestingly, exhibit a similar anomaly. Furthermore, we observe an important scaling law combining these two exponents.

The IM Hamiltonian can be written in the general form [1,7,14,15] $H = -(1/2)\sum_i \sum_{j \neq i} J_{ij} S_i S_j$, with J_{ij} being the strength of the interaction between two spins S_i and S_j ($= \pm 1$), sitting at the lattice points i and j . For $J_{ij} > 0$, one expects mostly parallel alignment of the spins at low-enough

^{*}das@jncastr.ac.in

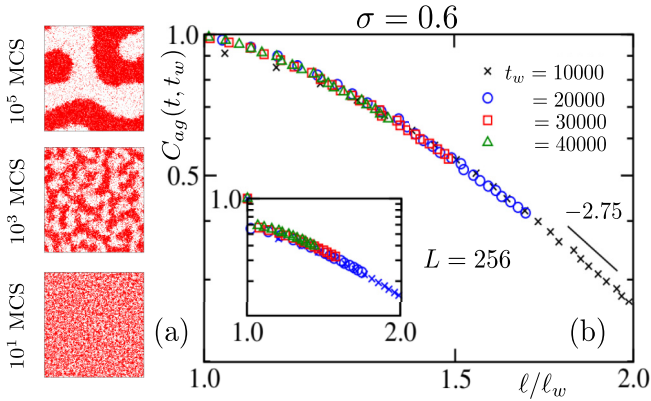


FIG. 1. (a) Evolution snapshots, starting from a random initial configuration, at different times, are presented for $L = 256$. (b) Plots of the autocorrelation function $C_{ag}(t, t_w)$ versus ℓ/ℓ_w , for several t_w . The inset contains the actual data. Results in the main frame are scaled by a pre-factor, after discarding the jumps, such that C_{ag} smoothly approaches 1, as $\ell/\ell_w \rightarrow 1$, for most of the t_w values. The solid line represents a power law. These results are for $\sigma = 0.6$.

temperatures. For standard purposes [1], one considers $J_{ij} = J$ and terminates the interaction at the nearest neighbor (NN) distance. For defining the LRIM, a power-law variation of the strength, as a function of r , the intersite distance, is considered [14,18]: $J_{ij} = J/r^{d+\sigma}$, with d being the spatial dimension and σ a constant. In the static critical phenomena, the value of σ , which separates the short-range and long-range universality classes, is close to 2 [13].

For conserved order-parameter dynamics the total numbers of $+1$ (or particles of type A) and -1 (or particles of type B) spins remain constant throughout the evolution. To ensure this, Kawasaki spin-exchange is used in our Monte Carlo (MC) simulations [22]. In this process, two (nearest) neighboring sites are randomly chosen, and in a trial move the corresponding spin states are exchanged that is accepted with certain probability following the Metropolis criterion [22]. For this purpose, the energy change needs to be calculated. With the Hamiltonian and the coupling term mentioned above, this calculation is demanding [19]. To minimize the computational cost, a generalized [23] Ewald summation [23,24] technique is used. We performed the calculations with (in-house) *parallel* codes, written with OPENMP and MPI, for even faster outputs. Spins are considered on periodic square lattices of size $L \times L$. For each σ , random initial configurations with equal concentrations of up and down spins are quenched to a temperature (T) that is 0.6 times the corresponding critical temperature [23]. At a finite temperature there exists noise in the structure. This was removed via a majority spin rule [10] for the calculation of length, which was obtained from the domain-size distribution [10]. All results are presented after averaging over a large number of initial configurations. We consider $L = 256, 512$, and 1024 with statistics over 175,100, and 8 initial configurations. Unless otherwise mentioned, we have $L = 256$. Time in our simulations is measured in units of MC steps (MCS), with one MCS being equivalent to L^2 trials.

In Fig. 1(a) we show evolution snapshots for $\sigma = 0.6$ from three different times. The locations of A particles are marked in red. In Fig. 1(b) we show a few plots of the autocorrelation function. The decay of C_{ag} is typically slower for an older system than a younger one, which reflects aging with passing time. This is a violation of the time-translation invariance and implies that in an “away from steady-state” situation, there is no scaling collapse of data for C_{ag} when results for different t_w are plotted versus $t - t_w$. This is unlike the steady-state situation. However, collapse is interestingly observed [2] when the data are plotted versus $x = \ell/\ell_w$, where ℓ_w is the value of ℓ at $t = t_w$. For $x \rightarrow \infty$, one then discusses the scaling behavior [2] $C_{ag}(t, t_w) \sim x^{-\lambda}$. In Fig. 1(b) we show C_{ag} with the variation of x . The original results are presented in the inset. The early period data, including the jumps, have a connection with the equilibration of the domain magnetization [7]. In the main frame the results are presented by discarding the jumps, keeping the data having a connection mainly with the growth of domains. We rescaled the ordinate after removing the points associated with the jumps. This way C_{ag} appears to approach unity, as $x \rightarrow 1$, in a continuous fashion, for several of the plots. This transformation does not alter the outcomes of the analyses below. It, in fact, brings better visual clarity over the relevant range from which it becomes easier to recognize the quality of collapse. A nice collapse of data for different t_w values is observed, despite certain difficulties associated with slow growth and delay in scaling due to settling time for the domain magnetization with the conserved order-parameter. It appears that, for the considered time range, we are reasonably away from any discernible finite-size effects [8–10]. In the finite-size affected situation data for different t_w should deviate from the master (collapsed) curve. The solid line in Fig. 1(b) represents a power-law with $\lambda = 2.75$. For large values of x , the simulation data are reasonably consistent with this line. However, to derive more accurate information, below we carry out certain advanced analyses.

We calculate an instantaneous exponent [2,8–10,25,26]: $\lambda_i = -d \ln C_{ag}(t, t_w)/d \ln x$. In Fig. 2(a) we present λ_i versus t_w/t for two values of σ . These show linear trends. The continuous lines are fits of the simulation data sets to the form $\lambda_i = \lambda + at_w/t$, with a being a constant. These provide $\lambda \simeq 2.86$ and $\lambda \simeq 3.15$, implying that the *aging exponents are nonuniversal*, having a dependence on the range of interaction. In Fig. 2(b), we show a plot of λ as a function of σ . We will reconfirm such dependence later by analyzing the data from systems with different L via multiple methods. We will also present results on the NN case to identify a crossover from the long- to short-range regime. To make the conclusion on crossover more accurate, we will study structure and growth as well.

We recall here certain lower bounds on λ , provided by Yeung, Rao, and Desai (YRD) [4]: $\lambda \geq (d + \beta)/2$. The derivation of this required integration of the equal-time structure factor $S(k, t_w)$ over k . It was noted that contribution only from small k was important at long times, for which $S(k, t_w) \sim k^\beta$ was assumed [27]. Since this power law is expected to be valid only for $k \rightarrow 0$, it is important to check the validity of the bound, particularly when λ exhibits a nontrivial σ dependence. For conserved dynamics in $d = 2$, $\beta = 4$ [27]. Thus, λ should be greater than 3, which is clearly not

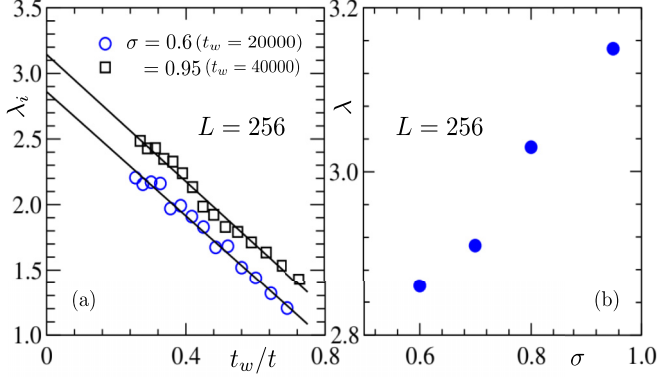


FIG. 2. (a) The instantaneous exponent λ_i is plotted versus t_w/t . Results from two σ values are shown. The solid lines are linear fits to the data sets. Since λ_i is a noisy quantity, running averaging was carried out for data smoothening. (b) The plot of λ , obtained from the fits in (a), versus σ . These were estimated by considering t_w values belonging to the scaling regime. For t_w/t closer to zero, there is the possibility of detectable finite-size effects. On the other hand, it becomes necessary to discard data very close to unity to avoid the time regime related to the stabilization of domain magnetization.

the case for the lower σ values. However, before drawing a conclusion on the violation of the YRD bounds, we take a look at the structural properties in Fig. 3. In Fig. 3(a), we show the structure factors from $L = 256$ and 512 for $\sigma = 0.6$. While the data for different system sizes agree with each other, the set from the larger system appears more useful with respect to the identification of the small k behavior. Before discussing β , however, we take a look at the large k behavior. In this limit, due to scattering from the interfaces,

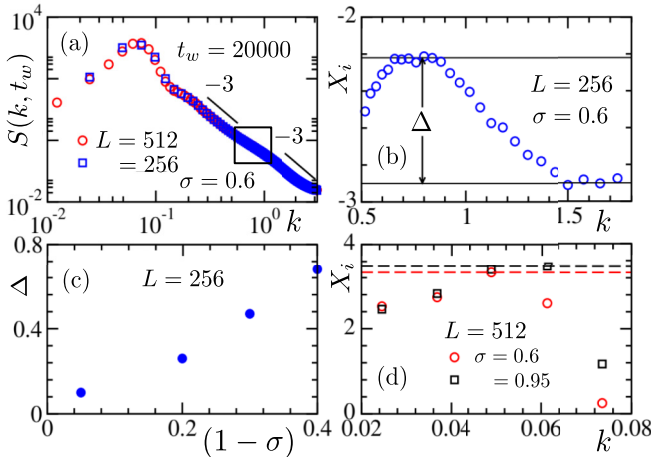


FIG. 3. (a) Structure factors, $S(k, t)$, at $t_w = 20000$, are plotted versus k for systems of different sizes with $\sigma = 0.6$. The solid lines represent power laws. (b) Instantaneous exponent X_i , for $L = 256$, is plotted versus k , for $\sigma = 0.6$. The upper horizontal line measures a maximum, corresponding to a knee, marked by a square in (a), and the lower one estimates the Porod exponent. (c) The differences between the maxima and the Porod exponent are plotted versus $(1 - \sigma)$. (d) X_i , for $\sigma = 0.6$ and 0.95 , with $L = 512$, are plotted versus k . The dashed lines indicate the locations of the small k maxima. The structure factors are taken from the scaling regimes of t_w .

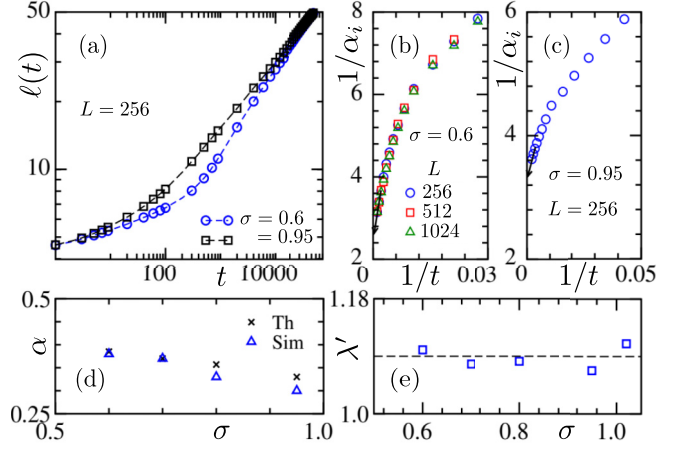


FIG. 4. (a) Log-log plots of $\ell(t)$ versus time, for $\sigma = 0.6$ and 0.95 . (b) The inverse of the instantaneous exponents, α_i , for $\sigma = 0.6$, versus $1/t$, for different L . The solid line is a guide to the eyes, showing possible convergence of the data sets in the $t \rightarrow \infty$ limit. We discard the noisy data at very late times (that may as well contain minor finite-size effects). This helps for better visualization of the convergences. (c) Same as part (b), but here we show results for $\sigma = 0.95$ and $L = 256$. For the calculation of α_i (also for X_i , λ_i , and λ'_i), original data are used to interpolate in equal abscissa intervals in log scales. (d) Plots of α as a function of σ . Results from both simulations (Sim) and theory (Th) are included. (e) Plot of $\lambda' (= \alpha\lambda)$, versus σ , by accepting the theoretical values for α . For $\sigma > 1$, we take $\lambda = 3.33$ that will be estimated from the simulations of the NN Ising model later for an arbitrary choice $\sigma = 1.02$.

one expects a Porod law [1], which, for the present case, should be $S(k, t) \sim k^{-3}$. Interestingly, for $\sigma = 0.6$, this behavior appears in two places, separated by a knee (see the bending between two power-law lines). This is absent in the short-range case. The appearance of this limits the observation of the Porod law continuously over a large range, despite the absence of finite-size effects. In Fig. 3(b), we show the instantaneous exponents $X_i = d \ln S(k, t) / d \ln k$ as a function of k for $\sigma = 0.6$. (It is a better practice to calculate such exponents instead of estimating a power-law exponent from a log-log plot.) The knee results in a maximum in X_i , at an intermediate k , before the final Porod behavior appears as a lower value close to -3 . (Note that at nonzero T the interfaces are less sharp and so the exponents usually are somewhat less than 3 .) We estimate Δ , the deviation of the maximum from the Porod exponent. In Fig. 3(c) Δ is plotted versus $(1 - \sigma)$. The data hint the disappearance of the knee as $\sigma \rightarrow 1$. This reflects the crossover discussed in the context of aging. Returning to the small k behavior, in Fig. 3(d) we show X_i for two different values of σ . Even if we consider the maxima in this figure as the true values of β , no violation of the YRD bound can be ascertained.

Previous estimates [9,28] of λ for nonhydrodynamic short-range interactions in $d = 2$ fall in the range $[3.3, 3.6]$. We will revisit this case, with better statistics, later in this work. The objective will be to verify if a convergence to the short-range case for λ is in agreement with the corresponding crossovers for structure and growth. A prediction for the latter states [14]: $\alpha = 1/(2 + \sigma)$, for $\sigma < 1$ and $\alpha = 1/3$, for $\sigma > 1$. A recent

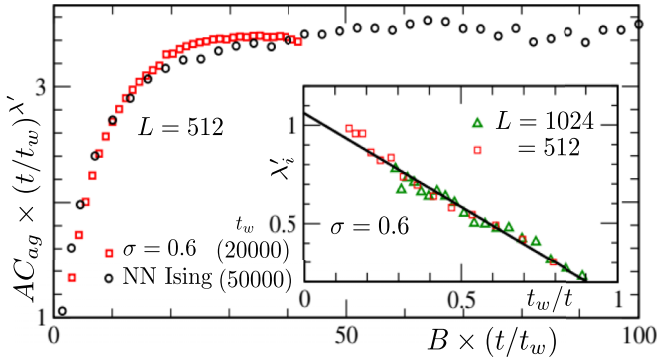


FIG. 5. $C_{ag} \times (t/t_w)^{\lambda'}$ is plotted versus t/t_w for $\sigma = 0.6$ and the NN model with $L = 512$. The constant prefactors A and B are introduced for visual convenience by facilitating better utilization of space inside the graph. Inset shows instantaneous exponent λ'_i , versus t_w/t for $\sigma = 0.6$ and multiple values of L . The solid line is a guide to the eyes.

computational study [16] showed consistency with this prediction. Nevertheless, we present the below simulation results on independent estimates of α . Note that no such predictions exist for λ . For this exponent, the existing predictions are only for the nearest-neighbor case with nonconserved dynamics [2,3]. For λ , not only are the theoretical calculations, but also the computer simulations and their analyses are challenging. This is more so for the long-range interaction, particularly for the conserved dynamics. Nevertheless, for a careful conclusion we will present results from larger systems and analyze our data using different methods.

In Fig. 4(a), we show log-log plots of ℓ versus t for $\sigma = 0.6$ and 0.95 . The growth, after early transients, appears stronger for the smaller value of σ . In Fig. 4(b) we show the instantaneous exponent for ℓ viz. $\alpha_i (= d \ln \ell / d \ln t)$, with the variation of t for $\sigma = 0.6$. To ascertain the absence of any influence of finite-size effects in our conclusions we show results from three system sizes. Each data set shows convergence to the same asymptotic value. In Fig. 4(c), we show similar data for $\sigma = 0.95$. In this case, we expect even weaker finite-size effects. Thus, we include data only for $L = 256$. These outcomes imply higher α for smaller σ . Corresponding plots are shown in Fig. 4(d). An interesting dependence can be recognized. There the theoretical values are also marked. Good agreement exists. In Fig. 4(e) we show λ' , the product

of α and λ , by accepting the theoretical values for α . It appears that $\alpha\lambda$ is independent of σ , the constant value equalling $\simeq 1.1$.

To reconfirm this conclusion, we analyze our aging data in different ways in Fig. 5 by using even larger systems. In the main frame we present $C_{ag}(t, t_w) \times (t/t_w)^{\lambda'}$, with $\lambda' = 1.1$, for $\sigma = 0.6$ and the NN model to show that at large enough t/t_w the ordinate is a constant, implying $\alpha\lambda \simeq 1.1$. We also calculate $\lambda'_i = -d \ln C_{ag} / d \ln(t/t_w)$ and identify its convergence when $t/t_w \rightarrow \infty$ for $\sigma = 0.6$ in the inset. There we show data from larger system sizes, including $L = 1024$. The convergence is toward $\lambda' \simeq 1.1$. These, combined with the corresponding outcomes for structure and growth, suggest that the above-mentioned crossover occurs at $\sigma = 1$. Note that this implies a short-range value of $\lambda = 3.33$ that is used in Fig. 4(e).

In conclusion, for the long-range Ising model [14], we presented results on aging and related phenomena, obtained via Monte Carlo simulations [22] in space dimensions two, for several values of the interaction-range parameter σ . It appears that with the increase of σ , the aging exponent λ increases. We compared the values of λ with the lower bounds predicted in Ref. [4]. The bounds are quite closely satisfied by all the obtained values. Our results for the structure and growth law are also consistent with the picture of the nonuniversality in aging. The boundary between the long- and short-range cases appears to be located around $\sigma = 1$. These are interesting deviations from the case of static critical phenomena, in terms of nonuniversality as well as the shifting of the boundary. The findings are important additions to the current developments in phase transitions [29,30], inviting further theoretical and confirmatory experimental studies on growth as well as aging. Interestingly, we observe that $\alpha\lambda$ remains a constant. This suggests that aging is more prominent in a quicker growing system. It will be important to carry out similar studies in different dimensions. Even if the growth part turns out to be trivial, we expect, guided by the lower bounds, λ to exhibit interesting dependence. An analogous investigation should be carried out for the nonconserved dynamics also. For a more global picture, different models, e.g., the q -state Potts model with long-range interaction, will prove useful. Long-range interaction in the presence of hydrodynamics should also be considered.

We acknowledge computation times in the Param Yukti supercomputer, located in JNCASR, under National Supercomputing Mission.

- [1] A. J. Bray, Theory of phase-ordering kinetics, *Adv. Phys.* **51**, 481 (2002).
- [2] D. S. Fisher and D. A. Huse, Nonequilibrium dynamics of spin glasses, *Phys. Rev. B* **38**, 373 (1988).
- [3] F. Liu and G. F. Mazenko, Nonequilibrium autocorrelations in phase-ordering dynamics, *Phys. Rev. B* **44**, 9185 (1991).
- [4] C. Yeung, M. Rao, and R. C. Desai, Bounds on the decay of the autocorrelation in phase ordering dynamics, *Phys. Rev. E* **53**, 3073 (1996).
- [5] M. Henkel, A. Picone, and M. Pleimling, Two-time autocorrelation function in phase-ordering kinetics from local scale invariance, *Europhys. Lett.* **68**, 191 (2004).
- [6] E. Lorenz and W. Janke, Numerical tests of local scale invariance in ageing q -state Potts models, *Europhys. Lett.* **77**, 10003 (2007).
- [7] M. Zanetti, in *Kinetics of Phase Transitions*, edited by S. Puri and V. Wadhawan (CRC Press, Boca Raton, FL, 2009).
- [8] J. Midya, S. Majumder, and S. K. Das, Aging in ferromagnetic ordering: Full decay and finite-size scaling of autocorrelation, *J. Phys.: Condens. Matter* **26**, 452202 (2014).
- [9] J. Midya, S. Majumder, and S. K. Das, Dimensionality dependence of aging in kinetics of diffusive phase separation: Behavior of order-parameter autocorrelation, *Phys. Rev. E* **92**, 022124 (2015).

- [10] N. Vadakkayil, S. Chakraborty, and S. K. Das, Finite-size scaling study of aging during coarsening in non-conserved Ising model: The case of zero temperature quench, *J. Chem. Phys.* **150**, 054702 (2019).
- [11] N. Vadakkayil, S. K. Singha, and S. K. Das, Influence of roughening transition on magnetic ordering, *Phys. Rev. E* **105**, 044142 (2022).
- [12] H. Christiansen, S. Majumder, M. Henkel, and W. Janke, Aging in the long-range Ising model, *Phys. Rev. Lett.* **125**, 180601 (2020).
- [13] M. E. Fisher, S. Keng Ma, and B. G. Nickel, Critical exponents for long-range interactions, *Phys. Rev. Lett.* **29**, 917 (1972).
- [14] A. J. Bray, Domain-growth scaling in systems with long-range interactions, *Phys. Rev. E* **47**, 3191 (1993).
- [15] A. J. Bray and A. D. Rutenberg, Growth laws for phase ordering, *Phys. Rev. E* **49**, R27 (1994).
- [16] F. Müller, H. Christiansen, and W. Janke, Phase-separation kinetics in the two-dimensional long-range Ising model, *Phys. Rev. Lett.* **129**, 240601 (2022).
- [17] R. Agrawal, F. Corberi, F. Insalata, and S. Puri, Asymptotic states of Ising ferromagnets with long-range interactions, *Phys. Rev. E* **105**, 034131 (2022).
- [18] F. Corberi, E. Lippiello, and P. Politi, One dimensional phase-ordering in the Ising model with space decaying interactions, *J. Stat. Phys.* **176**, 510 (2019).
- [19] H. Christiansen, S. Majumder, and W. Janke, Phase ordering kinetics of the long-range Ising model, *Phys. Rev. E* **99**, 011301(R) (2019).
- [20] J. C. Halimeh, M. Punk, and F. Piazza, Aging dynamics in quenched noisy long-range quantum Ising models, *Phys. Rev. B* **98**, 045111 (2018).
- [21] T. Ishihara and H. Hayakawa, Simulation of phase ordering kinetics in conserved scalar systems with long-range interactions, *Phys. Rev. E* **50**, 1629 (1994).
- [22] D. P. Landau and K. Binder, *A Guide to Monte Carlo Simulations in Statistical Physics* (Cambridge University Press, Cambridge, England, 2005).
- [23] T. Horita, H. Suwa, and S. Todo, Upper and lower critical decay exponents of Ising ferromagnets with long-range interaction, *Phys. Rev. E* **95**, 012143 (2017).
- [24] M. P. Allen and D. J. Tildesley, *Computer Simulation of Liquids* (Oxford University Press, Oxford, 1991).
- [25] D. A. Huse, Corrections to late-stage behavior in spinodal decomposition: Lifshitz-Slyozov scaling and Monte Carlo simulations, *Phys. Rev. B* **34**, 7845 (1986).
- [26] J. G. Amar, F. E. Sullivan, and R. D. Mountain, Monte Carlo study of growth in the two-dimensional spin-exchange kinetic Ising model, *Phys. Rev. B* **37**, 196 (1988).
- [27] C. Yeung, Scaling and the small-wave-vector limit of the form factor in phase-ordering dynamics, *Phys. Rev. Lett.* **61**, 1135 (1988).
- [28] F. Dittrich, J. Midya, P. Virnau, and S. K. Das, Growth and aging in a few phase-separating active matter systems, *Phys. Rev. E* **108**, 024609 (2023).
- [29] H. C. Chauhan, B. Kumar, A. Tiwari, J. K. Tiwari, and S. Ghosh, Different critical exponents on two sides of a transition: Observation of crossover from Ising to Heisenberg exchange in skyrmion host Cu_2OSeO_3 , *Phys. Rev. Lett.* **128**, 015703 (2022).
- [30] F. Meng, W. Liu, A. Rahman, J. Zhang, J. Fan, C. Ma, M. Ge, T. Yao, L. Pi, L. Zhang, and Y. Zhang, Crossover of critical behavior and nontrivial magnetism in the chiral soliton lattice host $\text{Cr}_{1/3}\text{TaS}_2$, *Phys. Rev. B* **107**, 144425 (2023).